Chapter 11
Luminescent Lanthanide Sensors and Lanthanide Doped Upconversion Nanoparticles: Current Status and Future Expectations

Garima Sharma, Preeti Sehgal, and Anudeep Kumar Narula

Abstract Lanthanide ions exhibit fascinating optical properties with their potential applications largely governed by their interaction with light. This chapter deals with some relevant aspects concerning the electronic and coordination properties of lanthanides and the basic principles related to the design of efficient luminescent lanthanide complexes. The cleverly designed environment consisting of ligands containing adequate chromophoric groups provide a rigid and protective coordination shell to minimize non-radiative deactivation. Lanthanide doped upconversion nanoparticles (UCNPs) have attracted extensive attention in the field of biomedical applications due to their long luminescence lifetime, narrow emission bandwidth, high quantum yields and low toxicity. In this chapter the upconversion phenomenon is explained with emphasis on the mechanism of upconversion, selection of host materials and impurities in host matrices. The various chemical approaches for the synthesis of lanthanide doped UCNPs have also been discussed. Subsequently, some selected results of our recent work concerning the photoluminescence studies of Eu(III) and Yb (III) complexes are reported which exhibit the characteristic emission bands of Eu(III) ion corresponding to $^5D_o \rightarrow {}^7F_J$ (J = 0–4) transitions with intense red emission at 615 nm due to $^5D_0 \rightarrow {}^7F_2$ transition of the central Eu(III) ion. These complexes show long radiative lifetime and quantum efficiency which suggest that these complexes can be well utilized as fluorescent probes.

Keywords Fluoroprobe • Energy transfer • Lanthanide complexes • Quanttum efficiency • Radiative lifetime

G. Sharma • P. Sehgal • A.K. Narula (✉)
University School of Basic and Applied Sciences, Guru Gobind Singh Indraprastha University, Delhi 110078, India
e-mail: researchchemlab58@gmail.com

C.D. Geddes (ed.), *Reviews in Fluorescence 2015*,
DOI 10.1007/978-3-319-24609-3_11

11.1 Introduction

The lanthanide complexes attract intense attention due to their superior optical properties and wide variety of potential applications i.e. biomedical assays and imaging, luminescence devices, ionic conductors and sensors. Majority of Ln^{3+} ions are luminescent, but some lanthanide ions are more emissive than others which depends on the feasibility of its excited state and non radiative de-activation paths. This can be achieved by sensitization through the surrounding ion and the overall quantum yield can be achieved by:

$$Q_{Ln}^{L} = \eta_{sens}\, Q_{Ln}^{Ln} \tag{11.1}$$

Where Q_{Ln}^{L} and Q_{Ln}^{Ln} are the quantum yields from indirect and direct transitions respectively while η_{sens} represents the efficiency with which electromagnetic energy is transferred from the surroundings to the metal ion [1]. The quantum yield for direct transition Q_{Ln}^{Ln} depends upon the energy gap between the emissive state of the metal ion and the highest sublevel of its ground multiplet. If this energy gap is small, the non radiative deactivation process will be faster. In lieu of above, some lanthanide ions such as Eu^{3+}, Gd^{3+} and Tb^{3+} ions are the suitable candidates with $\Delta E = 512{,}300$ ($^5D_0 \rightarrow {}^7F_6$), 32 200 ($^6P_{7/2} \rightarrow {}^8S_{7/2}$), 14,800 ($^5D_4 \rightarrow {}^7F_0$) cm^{-1} respectively. Out of above these, Gd^{3+} has potential applications for mercury free fluorescent lamps because under vaccum – UV excitation Gd^{3+} can efficiently transfer energy onto Eu^{3+} which results emission of two red photons also known as down conversion effect; but it is not very useful for bioanalysis because it emits in the UV region and its luminescence interferes with the emission or absorption process in organic part of complexes [2–6]. The advantages of Eu^{3+} and Tb^{3+} ions are their tunable energy gap with their sizes, therefore these two ions received much attention. Other lanthanides ions such as Sm^{3+}, Dy^{3+} have very low quantum yield hence they appear to be less useful in the applications of luminescence. Pr^{3+} emits both in visible and NIR regions and is considered a suitable component for optical materials because of its ability of generating up conversion process as well. Moreover, Nd^{3+}, Ho^{3+} and Yb^{3+} have found applications in the field of lasers and telecommunication devices because they emit in NIR spectral range. Nd^{3+} (lies at 1.06 nm) and Yb^{3+}(lies under 1 and 1.6 nm) are less useful than Pr^{3+} but act as an efficient sensitizer of Er^{3+} which emits at 1.55 nm [7, 8].

Recently, three ions Nd^{3+}, Er^{3+} and Yb^{3+} have gained popularity because technical developments occurred which facilitated the detection of weak NIR emissions for which efficient sensitizing groups have been explored.

11.2 Principle of Lanthanide Luminescence

The most interesting feature of these lanthanide series is their photoluminescence as these complexes show luminescence in visible or near infrared spectral region [9, 10]. The color of the emitted light depends upon the lanthanide ion viz. Eu^3

$^{+}$emits red light, Tb^{3+} emits green light, Sm^{3+} orange light, Tm^{3+} blue light. Pr^{3+}, Sm^{3+}, Dy^{3+}, Ho^{3+}, Tm^{3+} shows transitions in the near infrared region while Yb^{3+}, Nd^{3+}, Er^{3+}emits near infrared luminescence. Gd^{3+} luminescence can be observed in absence of organic ligands as it emits in ultraviolet region. In lanthanides, the emissions are due to f-f transitions [11, 12]. The partially filled 4f shell is shielded by $5s^2$ and $5p^6$ orbitals and the ligands in the first and second coordination sphere perturb the coordination sphere of lanthanide ions. The narrow band emission and long lifetimes of excited states of lanthanides is observed due to this shielding. Ce^{3+} is a unique case among all lanthanides due to f-d transitions. The emission maxima largely depends upon the ligand environment around Ce^{3+} ion [13–15].

All the lanthanide ions suffer from weak light absorption as the molar absorption coefficients of most of the transitions are smaller than 10 L $mol^{-1}cm^{-1}$ and a limited amount of radiations is absorbed by direct excitation in the 4f levels because luminescence intensity is proportional to quantum yield and the amount of light absorbed, weak light absorption results in weak luminescence. However, this can be overcome by the antenna effect. Weissman [16] found that upon excitation of lanthanide complexes with organic ligands, intense metal centered luminescence can be observed due to intense absorption of organic chromophores. The excitation energy is transferred from ligand to lanthanide ion via intramolecular energy transfer [17–20]. The same phenomena for the europium complexes with salicylaldehyde, benzoylacetone, and dibenzoylmethane and meta- nitro benzoylacetone has been described.

The mechanism of energy transfer from organic ligands to lanthanide ions is proposed by Crosby and Whan [21]. Upon ultraviolet irradiation, the organic ligands of the complexes are excited to a vibrational level of first excited singlet state (S_1 or S_0), then molecule undergoes to lower vibrational level of S_1 state via internal conversion. The excited singlet state can be deactivated to the ground state ($S_1 \rightarrow S_0$) or can undergo nonradiative intersystem crossing from singlet state S_1 to triplet state T_1. The triplet state T_1 can be radiatively to the ground state S_0 by spin forbidden transitions $T_1 \rightarrow S_0$. The complex may undergo indirect excitation by a non radiation transition from the triplet state to an excited state of the lanthanide ion which may undergo a radiative transition to a lower 4f state by photoluminescence or may be deactivated by non radiative process [22–28]. According to them, vibronic coupling of lanthanide with the ligand and solvent molecule is the main cause of non radiative deactivation of the lanthanide ion (Fig. 11.1).

However, a mechanism was proposed for energy transfer from excited singlet state S_1 to the energy levels of the lanthanide ions. But this theory is not of great importance because it is not efficient due to short lifetime of the singlet excited state [29]. This type of excitation is seen in Tb^{3+} and Eu^{3+}. Luminescence by the lanthanide ions is done by resonance levels. The main resonance levels are $^4G_{5/2}$ for Sm^{3+} ion (17,800 $cm^{-1)}$, $^5D_0$ for Eu^{3+}ion (17,250 cm^{-1}), $^5D_4$ for Tb^{3+} (20,430 cm^{-1}) and $^4F_{9/2}$ for Dy^{3+} (20,960 cm^{-1}) [30]. If the lanthanide is excited to a non emitting level either by direct excitation or indirect excitation, the excitation energy is dissipated via non radiative processes. To achieve the resonance level of the lanthanide, it is mandatory that the lowest triplet state of the

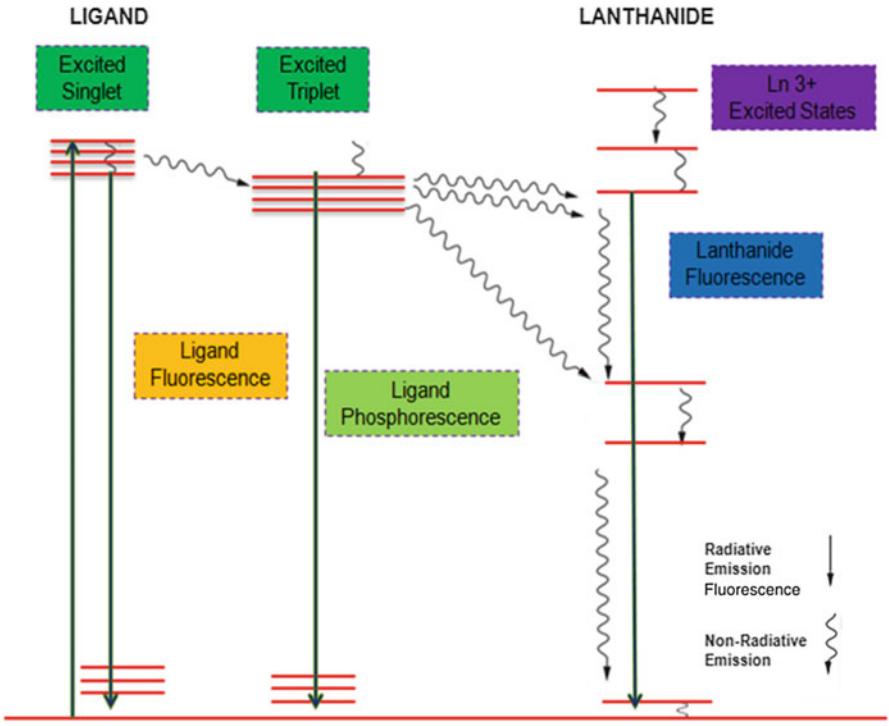

Fig. 11.1 Jablonski diagram representing the energy transfer in lanthanide complexes [28, 29]

complex is located at or equal to the resonance level of the lanthanide ion; if the energy levels of the organic ligands are present below the resonance level of lanthanide, molecular fluorescence or phosphorescence of the ligand is observed. Therefore it is a sensitive function of the lowest triplet level of the complex relative to a resonance level of the lanthanide ion [31–33].

Thus by the variation of ligands, it is possible to control the luminescence intensity for a given lanthanide ion, as the position of the triplet level depends on the nature of the ligands. Further, it is also temperature dependent, the luminescence caused by direct excitation of 4f level is less temperature sensitive than the luminescence caused by indirect excitation by organic ligands. The metal centered emission cannot be observed in case of Gd^{3+} ion as its 4f levels are located above the triplet levels. The presence of heavy paramagnetic ion results in mixing of triplet and singlet states and thereby enhancing the intersystem crossing from singlet state to triplet state [34]. The spin orbit coupling interaction helps the triplet state to acquire a partially singlet character which results in relaxation of selection rules.

The efficiency of energy transfer depends upon the overlap between the phosphorescence spectrum of the ligand and absorption spectrum of lanthanide ion. The back energy transfer can occur from the emitting 4f level of the lanthanide ion to the

triplet state of the ligand, if the energy match between these is very close to each other [35]. The fluorescence and phosphorescence of the ligands are quenched if there is efficient energy transfer from ligand to lanthanide ion, but if the energy transfer is not effective it results in observation of ligand emission in addition to the lanthanide emission.

The energy transfer through charge transfer states is another possibility of lanthanide luminescence. In this case, the light is absorbed by the ligand to metal charge transfer states (LMCT) from where the energy can be transferred to the 4f levels of the lanthanide ion, if the LMCT state lies high enough to the lanthanide 4f level. Eu^{3+} ion shows an efficient sensitization through charge transfer state if the LMCT lies above 40,000 cm^{-1} [36]. If this energy gap is low it results in the quenching of luminescence and when this energy gap is lower than 25,000 cm^{-1} it leads to total quenching.

11.3 Design of Luminescent Lanthanide Complexes

11.3.1 General Criteria

The lanthanide ions need a cleverly designed environment which consists of ligands containing adequate chromophores, harvesting light and simultaneously providing a rigid and protective coordination shell to minimize non-radiative deactivation. The laporte-forbidden f-f transitions have weak oscillator strengths which results in quenching by the high energy oscillators such as O-H, N-H or C-H groups located in the inner and outer coordination spheres [37]. The design of luminescent lanthanide complexes requires particular care as the electronic, magnetic and photo physical properties of Ln(III) complexes strongly depends on the control of the coordination sphere of the metal. Among various parameters which govern the control over chemical, structural and thermodynamical properties of the complex are ligand topology, (dimensionality, connectivity, shape, size and chirality) and binding sites (electronic properties, nature, number, shape and arrangement), layer properties (rigidity/flexibility and lipophilicity/hydrophilicity ratio, thickness), environment properties and the nature of counter ions present [38]. The luminescent Ln(III) complex represents a multi-component system organized as a supramolecular structure comprising of metal cation and antenna. In general, the complex formation results from the attraction of ligand and metal ion, the resulting complex then undergoes partial to total desolvation [39]. The coordination of lanthanide ion with the ligand is substantially based on the Van der Walls electrostatic forces of attraction. These type of interactions are also observed in alkali-earth cations particularly Ca^{2+}. The ligand interacts with the surface of metal cation thus replacing the first solvation sphere either partially or totally. The desolvation step shows an increase in entropy however the enthalpy variation can be positive or negative which can be attributed to the difference in the energy of the bonds formed

and the energy of the bonds broken between ligand and cation with solvent respectively [40]. In the complexation of Ln(III) in aqueous solution the dehydration step is endothermic ($\Delta H > 0$) which is an unfavourable energy contribution to the Gibbs free energy [41]. Therefore it is suggested to use polydentate ligands which show chelate effect and afford highly stable complexes in aqueous medium. In order to achieve the overall sensitization efficiency, the design of lanthanide complexes need certain factors to be considered which can be summarized as follows:

11.3.2 Choice of Lanthanide

The lanthanide ions show unique emission properties that cover the ultraviolet (Gd^{3+}) to the visible range (Sm^{3+}, Eu^{3+}, Dy^{3+}, Tb^{3+} and Tm^{3+}) and the near infrared range (Yb^{3+}, Nd^{3+} and Er^{3+}). The selection of the lanthanide ion depends on the intrinsic quantum yield which in turn depends on the energy gap between the lowest lying excited emissive state of metal ion and the highest sublevel of its ground multiplet. Accordingly, Eu^{3+}, Tb^{3+} and Gd^{3+} ions serve as good candidates for luminescent probes with energy gap values of 12,300 cm^{-1}, 14,800 cm^{-1} and 32,200 cm^{-1} however Gd^{3+} emits in ultraviolet region and used as contrast agents. The lanthanide ions possess relatively long lived excited states (microseconds to milliseconds) which can undergo energy transfer to high frequency vibrational oscillators such as O-H, N-H and to a lower extent C-H [42]. As a consequence, the presence of these groups in the proximity of the metal favours thermal dissipation of the energy (vibronic coupling) which gives rise to quenching of the luminescence (Fig. 11.2).

11.3.3 Choice of the Antenna

The term "antenna" refers to the chromophore which promotes the sensitization of lanthanide ion. It can be any aromatic or heteroaromatic highly π-conjugated system characterized by high efficiency of light absorption and high efficiencies of intersystem crossing and energy transfer process. The high yield of energy transfer from the antenna to the metal ion occurs until certain conditions are satisfied such as nature of ion, electronic structure of the donor, their relative positioning and the nature of interaction between metal ion and ligand [43]. The ligand geometric and electronic structure must be taken into account for various energy transfer pathways resulting from energy levels such as singlet $^1S_i (i = 1,2)$, triplet ^3T, intra ligand charge transfer (ILCT), ligand to metal charge transfer (LMCT). Generally, these energy pathways terminate at the emissive level of the lanthanide ion. The potential donor levels of the antenna should be chosen such that these are reasonably above the Ln(III) emissive level to avoid back transfer and is

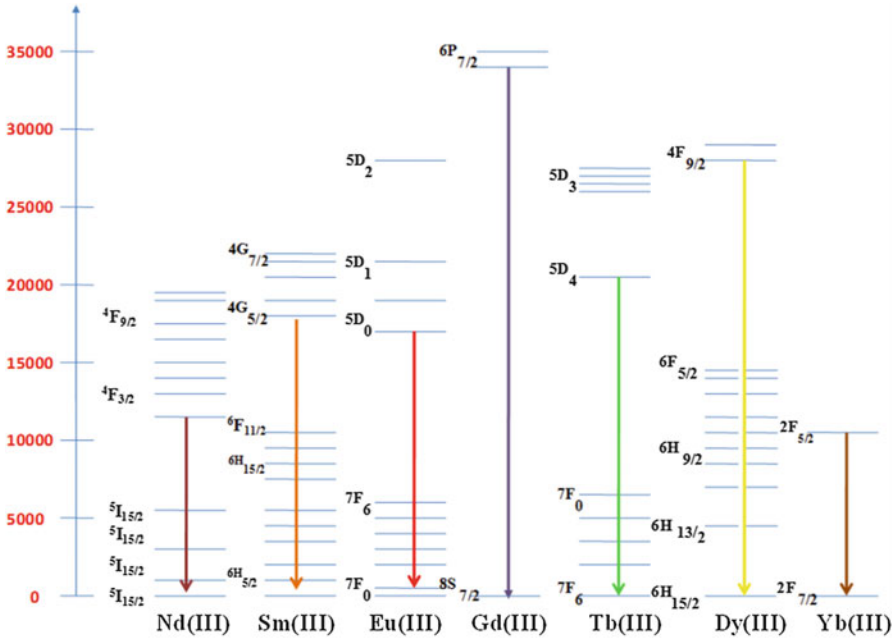

Fig. 11.2 Energy level diagram for the Ln(III) ions showing the main emitting levels and the transitions to the ground state levels [42]

close resonance with one of the higher 4f states. This energy gap should be atleast 1850 cm^{-1} higher than the lowest emitting level of Ln(III) ion. At higher value, the energy transfer from the triplet flows through the non-radiative excited state of the metal until it reaches the emissive levels and metal centered emission occurs. However, at lower energy gap strong thermal deactivation takes place due to back energy transfer and O_2 –quenching towards the chromophore triplet level [44]. The triplet state energies of some of the commonly used chromophores are reported in Table 11.1. The dependence of the luminescence of Ln(III) ion on the excitation wavelength also suggests that it should be above ca. 350 nm to facilitate the use of inexpensive excitation sources.

The lanthanides do not have restricted coordination number and geometry, these can therefore extend their coordination number ranging from 3 to 12, although 8 and 9 are considered the most common ones [46]. This property can be utilized by several auxillary N-or O- donor co-ligands for coordination and to make saturated complexes. In such complexes, the energy transfer is more effective from ligand to metal and complexes show intense photoluminescence which can be attributed to the increased anisotropy around the lanthanide ion. The introduced auxillary coligands make the complex more rigid and asymmetric around the central metal ion which overall improve the photophysical properties of the complexes [47]. The photophysical properties can also be tuned by substituting releasing or donating groups at various positions of the coordinated neutral auxillary ligands. The

Table 11.1 Energy levels of some commonly used chromophores [45]

Chromophore	Singlet (cm^{-1})	Triplet (cm^{-1})
1,10 Phenanthroline	29,200	22,100
Acetophenone	28,200	26,000
1,4-Napthoquinone		20,200
8-Hydroxyquinone	27,000	
7-Amino-4-methyl-2- hydroxyquinone		23,100
Tetrazatriphenylene	29,000	24,000
Napthalene	32,200	21,200
2-Hydroxyisophthalamide	24,200	23,350
1-Hydroxy pyrin-2-one		21,260

N-donor neutral auxillary ligands are 1,10-phenanthroline (phen), 2,2′-bipyridine (bipy), terpyridine (terpy) and their analogues form stable ternary complexes with wide range of 1:3 neutral lanthanide complexes [48–52]. The 1,3-diketonate tris complexes and adducts with some auxillary coligands explained the structural behavior of the coligand and its effect towards luminescence intensity stating that a rigid planar structural ligand behaves better in effective energy transfer which is further supported by the comparative study of $Eu(tta)_3$.phen and $Eu(tta)_3$.bipy. The important factor to choose a neutral ligand to enhance photoluminescence properties of lanthanides is the value of excited energy levels (singlet and triplet) of the corresponding auxillary ligand [53]. The corresponding singlet and triplet energy levels of bipy(29,900 cm^{-1}, 22,900 cm^{-1}) and phen(31,000 cm^{-1}, 22,100 cm^{-1}) were found suitable for effective energy transfer from ligand to metal and exhibit enhanced metal centered luminescence [54].

1,10-phenanthroline ligand behaves as a weak base in aqueous solution, the protonation constant being 4.95 log units. Its basicity is remarkably lower than aliphatic diamines, such as ethylenediamine(log k = 10.65 and 8.05 for successive addition of acidic protons) which shows its lower donor ability of its nitrogen atoms. [55] Compared to the parent 2,2′-bipyridine (bipy) and 2,2′,6′,6″ terpyridine systems, phen is characterized by two inward-pointing nitrogen donor atoms and therefore pre-organized for strong and entropically favoured metal binding [56]. The photophysical properties of phen have been a subject of a number of studies. Phen is characterized in aqueous solution by UV absorptions at 229 nm and 265 nm, the latter attributed to the $\Pi \rightarrow \Pi^*$ transition to the lowest energy excited singlet state. Excitation at 307 nm originates a fluorescence emission band at 380 nm, due to radiative decay of $\Pi \rightarrow \Pi^*$ state. These spectroscopic features are modulated by appropriate substituents on the phen framework and pH changes i.e. by protonation of the heteroaromatic nitrogen atoms. The UV-spectrum recorded at pH 4, where phen is monoprotonated form, $(phenH)^+$ shows the absorbance 8 nm red shifted to the absorption band at 265 nm attributed to the charge transfer of the $\Pi \rightarrow \Pi^*$ transition(i.e. the LUMO has a higher electron density on the nitrogen atoms than the HOMO. Monoprotonation of phen leads to the disappearance of the emission band at 380 nm and to the formation of a new

emission broad red shifted band at ca. 410 nm accounting for stabilization of lowest energy state by protonation of the heteroaromatic nitrogen atoms because of its charge transfer character [57]. The electron deficiency of chelating agents phen and bipy is their electron deficiency that makes them excellent acceptors capable of stabilizing metal ions in lower oxidation states. Due to the presence of low energy Π* orbitals of the ligand, metal complexes can be characterized by strong metal-to-ligand charge transfer (MLCT) absorption bands in the visible spectrum and red shifted fluorescent emissions.

Another major class of co-ligands are phosphine oxides and their analogues which are widely studied and used as sensitizers now. The disappearance of broad absorption band in the region of 3000 cm^{-1} in the IR spectra of lanthanide ternary complexes of pyrazolonates confirms the substitution of water coordination by various phosphine oxide ligands. The increase in photoluminescence intensity of phosphine oxides coordinated Eu(III) complexes can be due to square antiprismatic structures of the complexes which promotes faster radiation rates and an increase in $^5D_0 \rightarrow {}^7F_2$ emissions related to odd parity. The substitution of auxillary sensitizing ligands in lanthanide complexes also increases the solubility of complexes in organic solvents depending on the substituted neutral ligand used.

The above discussion concludes that the ligand topology, binding sites, layer properties, and environment properties of the antenna plays an important role in the design of lanthanide complexes. In addition to this, the radiative lifetime and photoluminescence quantum yield of lanthanide complexes also influence the design of luminescent sensors.

Among the organic ligands, the pyridine derivatives are important as they form a diversity of coordinating structures including coordination polymers and also have numerous applications in catalysis, non linear optics, luminescence, ion exchange, material chemistry and magnetochemistry, the role of 1,10-phenanthroline as an auxillary ligand is well known and plays a significant role in absorption and transfer of energy to the emission center Eu(III) ion [58–60]. The auxillary ligand reduces the non radiative decay of the excited states of Eu(III) ion and increase the energy transfer efficiency from ligands to Eu(III) ion thereby increasing the stability of europium complexes. Similar observations have been made with the europium complexes $[Eu(2\text{-ap})_3(phen)]Cl_3$**(1)**, $[Eu(2\text{-ap})_2(phen)_2]Cl_3$**(2)** and $[Eu(2\text{-ap})(phen)_3]Cl_3$**(3)** synthesized with 2-aminopyridine and 1,10-phenanthroline ligands in different molar ratios [61] (Fig. 11.3).

The complexes exhibited characteristic emissions of Eu(III) ion at around 537 nm, 592 nm, 615 nm, 652 nm and 700 nm. These five expected bands are attributed to the $^5D_o \rightarrow {}^7F_J$ (J = 0–4) transitions of Eu(III) ion. The emission bands at 537 nm and 652 nm are very weak since their corresponding transitions $^5D_o \rightarrow {}^7F_o$ and $^5D_o \rightarrow {}^7F_3$ are forbidden in both magnetic dipole and electric dipole fields. The relative emission of $^5D_o \rightarrow {}^7F_1$ transition at 592 nm are relatively strong as it is a magnetic dipole transition which is independent of the coordination environment of Eu(III) ion. The $^5D_o \rightarrow {}^7F_2$ transition at 615 nm is an induced electric dipole transition which is very sensitive to the coordination environment of the Eu(III) ion. This transition is responsible for the strong red emission of

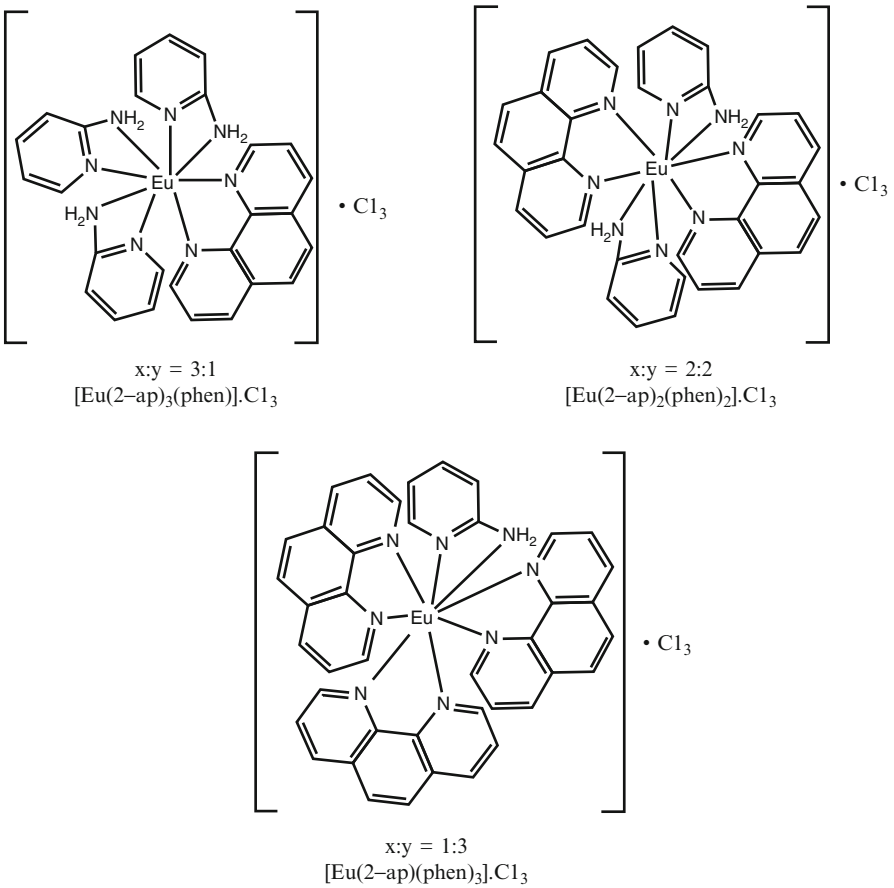

Fig. 11.3 Structure of europium complexes $[Eu(2\text{-ap})_3(phen)]Cl_3$(1), $[Eu(2\text{-ap})_2(phen)_2]Cl_3$(2) and $[Eu(2\text{-ap})(phen)_3]Cl_3$ (3) (x = 2-aminopyridine, y = 1,10-phenanthroline) [61]

europium complexes and also indicates the presence of highly polarizable chemical environment around the Eu(III) ion. The band at 700 nm is relatively weak and corresponds to the $^5D_o \rightarrow {}^7F_4$ transition. It was also noted that in all the three complexes, the intensity ratio of $^5D_o \rightarrow {}^7F_2$ transition to $^5D_o \rightarrow {}^7F_1$ transition was around 4.0 which indicated the location of Eu(III) ion in the environment of low symmetry. The presence of only one line for $^5D_o \rightarrow {}^7F_o$ transition revealed the presence of similar chemical environment around Eu(III) ion. The photoluminescence results showed that the relative emission intensity of $^5D_o \rightarrow {}^7F_2$ transition was enhanced as the molar ratio of the ligand phen increased from complex **(1)** to complex **(3)** which revealed that the sensitization ability of ligand phen is better than that of ligand 2-ap (Fig. 11.4).

The decay profile of complex **(3)** shows monoexponential function indicating the presence of a single chemical environment around Eu(III) ion. The lifetime value

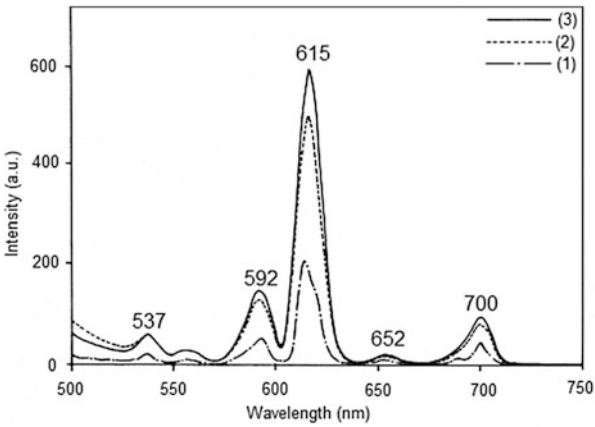

Fig. 11.4 Photoluminescence emission spectra of europium complexes in methanol solution (1×10^{-5} mol dm^{-3})$[Eu(2\text{-}ap)_3(phen)]Cl_3$ (1), $[Eu(2\text{-}ap)_2(phen)_2]Cl_3$ (2) and $[Eu(2\text{-}ap)(phen)_3]Cl_3$ (3) at the excitation wavelength of 247 nm [61]

was found to be 324 μs. According to the emission spectra and the lifetime of the Eu (III) excited state ($^5D_0$), the emission quantum efficiency (η) was found to be 10.33, which is good for a ligand-sensitized luminescent europium(III) complex (Fig. 11.5).

The above results indicate that the europium complex $[Eu(2\text{-}ap)(phen)_3]Cl_3$ with higher molar ratio of ligand 1,10-phenanthroline shows high luminescence as compared to other complexes $[Eu(2\text{-}ap)_3(phen)]Cl_3$ and $[Eu(2\text{-}ap)_2(phen)_2]Cl_3$. The quantum efficiency is found to be 10.33 which suggest the complex can act as a good fluorescent probe.

The pyridine carboxylates act as good candidates due to existence of N and O mixed donor atoms which can coordinate to the metal ion in a bidentate chelating, bidentate bridging and unidentate manner [62–64]. 2,6-pyridinedicarboxylic acid and α-picolinic acid have been found as promising ligands due to the stability of their Ln(III) complexes, strong fluorescence intensity with long excitation lifetimes [65–68]. The ligand 2,6-pyridinedicarboxylic acid is water soluble, commercially available having nitrogen and oxygen atoms to coordinate with the metal ion. Aminopyridine ligands also act as useful chelating agents for inorganic and organometallic applications and their derivatives can coordinate to the metal ions in a monodentate fashion through the N atom of the ring, however there are several works reported where the amino group also participates in coordination to the metal ion. The hydroxypyridine ligands can also coordinate effectively to the metal ion through the N and O donor atoms and are expected to show good luminescent properties [69–71]. The europium complexes $[\{Eu(dpa)(\alpha\text{-}pc)(CH_3OH)].2CH_3OH\}]$**(4)**, $[\{Eu(dpa)(2\text{-}ap)(CH_3OH)].2CH_3OH\}]$**(5)** and $[\{Eu(dpa)(2\text{-}hp)(CH_3OH)].2CH_3OH\}]$**(6)** with dipicolinic acid (dpa) as a primary ligand and α-picolinic acid (α-pc), 2-aminopyridine (2-ap) and 2-hydroxypyridine (2-hp)

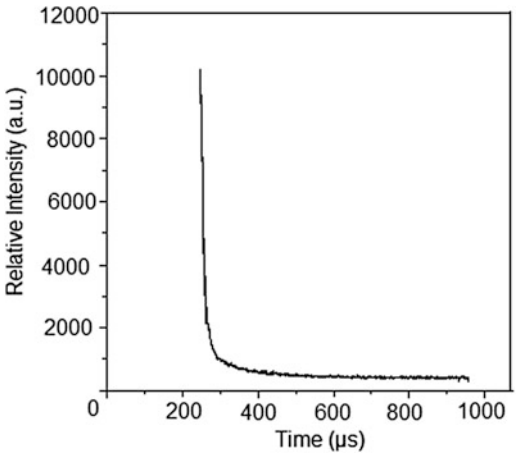

Fig. 11.5 Photoluminescence decay curve under laser pulse excitation of [Eu(2-ap)$(phen)_3$]Cl_3 complex [61]

as secondary ligands [72] shows strong characteristic emission bands of Eu(III) ions in the visible region, which attributes to the electronic transitions from the excited ^5D_o level to the ground ^7F_J (J = 0–4) levels of Eu(III) ion . The relative luminescent intensity of $^5D_o \rightarrow {}^7F_2$ transition is strongest in the complex based on 2-ap as secondary ligand, however the weakest luminescent intensity is observed in complex with 2-hp as secondary ligand. This can be explained by the non-radiative deactivation of energy of excited state as a result of their interaction with high frequency oscillators O-H group which act as efficient quencher of lanthanide ion luminescence in 2-hp ligand. These results showed that $–NH_2$ group in 2-ap ligand can strongly sensitize the luminescence of Eu(III) ion as compared to the 2-pc and 2-hp ligands (Fig. 11.6).

The luminescence decay curves of the complexes obtained at 298 K by monitoring the $^5D_0 \rightarrow {}^7F_2$ transition (615 nm) show monoexponential function indicating the presence of a single chemical environment around Eu(III) ion. The lifetime values are found to be 725 μs, 825 μs and 675 μs and the quantum efficiency values are found to be 21.60, 27.30 and 17.89 for complexes **(4)**, **(5)** and **(6)** respectively (Fig. 11.7).

The complexes show the characteristic emission bands of Eu(III) ion in visible region at 580 nm, 592 nm, 615 nm, 650 nm and 698 nm for $^5D_0 \rightarrow {}^7F_J$ (J = 0–4) transitions respectively. The photoluminescence properties of the complexes are influenced by the secondary ligands as studied by the photoluminescence spectra and decay measurements where the complex [{Eu(dpa)(2-ap)(CH_3OH)].$2CH_3OH$}] with 2-ap as secondary ligand exhibits strongest emission intensity and relatively longer luminescence lifetime, quantum efficiency as compared to the complex [{Eu(dpa)(α-pc)(CH_3OH)].$2CH_3OH$}] and complex [{Eu(dpa)(2-hp)(CH_3OH)].$2CH_3OH$}] (6).

Recently, the luminescent materials with the emissions in the near- infrared region such as Sm(III), Dy(III), Pr(III), Ho(III), Yb(III), Nd(III) and Er(III) have gained much interest due to their applications in telecommunication network as optical

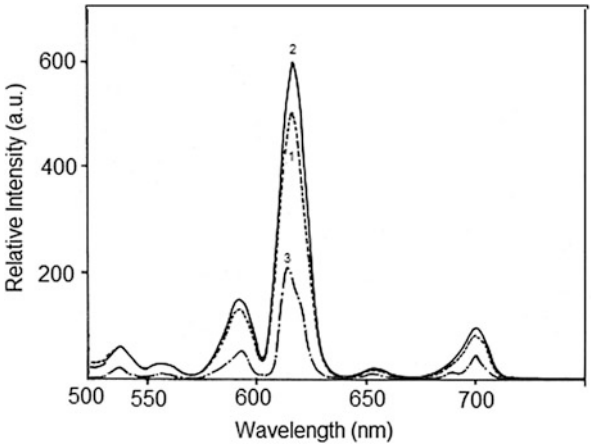

Fig. 11.6 Luminescent emission spectra of [{Eu(dpa)(α-pc)(CH_3OH)].2CH_3OH}] (4), [{Eu(dpa)(2-ap)(CH_3OH)].2CH_3OH}] (5) and [{Eu(dpa)(2-hp)(CH_3OH)].2CH_3OH}] (6) [72]

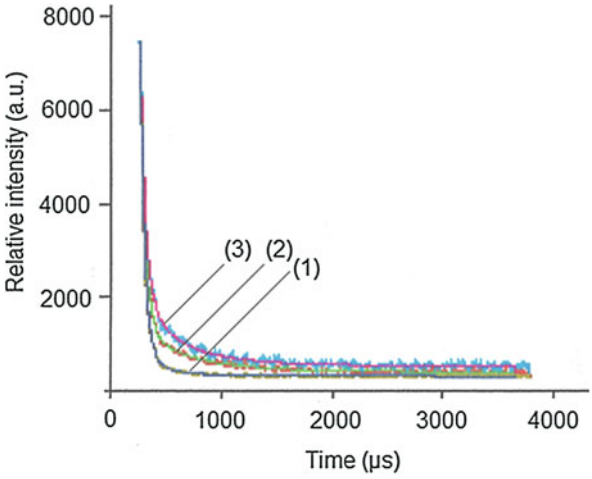

Fig. 11.7 Photoluminescent lifetime decay measurement of [{Eu(dpa)(α-pc)(CH_3OH)].2CH_3OH}] (4), [{Eu(dpa)(2-ap)(CH_3OH)].2CH_3OH}] (5) and [{Eu(dpa)(2-hp)(CH_3OH)].2CH_3OH}] (6) [72]

signal amplifier, probes for bioassays because human tissue is relatively transparent to near infrared light at 1000 nm. Yb^{3+} ion is usually a prime candidate to be chosen due to its luminescent efficiency close to 100 % and relatively simple electronic structure of two energy level manifolds: the $^2F_{7/2}$ ground state and $^2F_{5/2}$ excited state around at 10,000 cm^{-1} in the NIR region [73–77]. The rare earth ion couples such as RE^{3+}-Yb^{3+} can be efficiently utilized for near infrared (NIR) quantum cutting (QC) materials [78–80]. The energy gap of $^5D_2$ – $^7F_0$ transition in Eu^{3+} is approximately twice as large as that of $^2F_{5/2}$ – $^2F_{7/2}$ transition in Yb^{3+} which facilitates the energy transfer between Eu^{3+} ion to Yb^{3+} ion [81]. The room temperature excitation spectra of complex [$Eu_{0.5}Yb_{0.5}$ $(sal)_3$(phen)] [82] obtained by monitoring the longest

emission wavelength of Eu^{3+} ion at 614 nm and Yb^{3+} ion at 980 nm exhibits a broad band at 290 nm attributable to the ligand to metal charge transfer (CT) transitions caused by the interaction between the organic ligands and the Eu^{3+} ions at 614 nm . The strong absorption band centered at 261 nm corresponded to the ligand to metal charge transfer transitions of Yb^{3+} ions. The presence of relatively strong CT absorption band in the excitation spectrum of Yb^{3+} ions reveals the energy transfer from Eu^{3+} ions to Yb^{3+} ions. The excitation spectrum also shows the sharp 4f-4f transitions of Eu^{3+} from the $^7F_0$ ground state to $^5D_{3,4,6,7,1,2}$ excited states. The difference in energy between the $^5D_2 - {}^7F_0$ transition of Eu^{3+} ions is twice the energy difference between $^2F_{5/2} - {}^2F_{7/2}$ transition of Yb^{3+} ions, which means that the $^5D_2$ excited state of Eu^{3+} ion can simultaneously transfer energy to two nearby Yb^{3+} ions and hence the Yb^{3+} ions can emit two infrared photons. This absorption is followed by rapid multi-phonon assisted relaxation from the populated $^5D_2$ energy levels to the metastable energy levels of Eu^{3+} ion (Fig. 11.8).

The emission spectra obtained by the excitation at 384 nm, it was observed that the complexes $[Eu(sal)_3(phen)]$ and $[Eu_{0.5}Yb_{0.5}(sal)_3(phen)]$ show the characteristic narrow emission peaks corresponding to the $^5D_0 - {}^7F_j$ ($J = 0$–4) transitions of Eu^{3+} ions. The emission peaks are well resolved and it was observed that the peak at 578 nm and 650 nm were weak since their corresponding transitions $^5D_0 - {}^7F_0$ and $^5D_0 - {}^7F_3$ were forbidden in magnetic and electric dipole fields. The peak at 591 nm is relatively strong and corresponds to $^5D_0 - {}^7F_1$ magnetic transition, the strongest emission observed at 614 nm ($^5D_0 - {}^7F_2$) is an induced electric dipole transition sensitive to the coordination environment of Eu^{3+} ion. This transition was responsible for the red emission of the europium complexes. The relative intensity of peaks are stronger in complex $[Eu(sal)_3(phen)]$ as compared to complex $[Eu_{0.5}Yb_{0.5}(sal)_3(phen)]$. The decrease in intensity of all the emission peaks in complex can be considered due to the energy transfer from Eu^{3+} ions to Yb^{3+} ions in the complexes. The emission spectrum of complex $[Yb(sal)_3(phen)]$ which exhibits near infrared emission peaks at 980 and 1030 nm associated with the transition of Yb^{3+} from $^2F_{5/2}$ level to $^2F_{7/2}$ energy level. The decay curve shows the lifetime quenching of Eu^{3+} emission due to the energy transfer from Eu^{3+} to Yb^{3+} with mean lifetime of 461 ps (Figs. 11.9, 11.10, and 11.11).

The above results show the study of excitation, emission and decay measurements of $[Eu_{0.5}Yb_{0.5}(sal)_3(phen)]$ complex which reveals the efficient energy transfer from Eu^{3+} to Yb^{3+} by cooperative energy transfer process, which leads to Eu^{3+} emission quenching and occurrence of near infrared emission at 980 and 1030 nm.

11.3.4 Photoluminescence Quantum Yield and Radiative Lifetime

The most important feature of luminescent lanthanide complexes is the photoluminescence quantum yield (PLQY). It is defined as the ratio of number of photons emitted with that of number of photons absorbed when excited at a particular

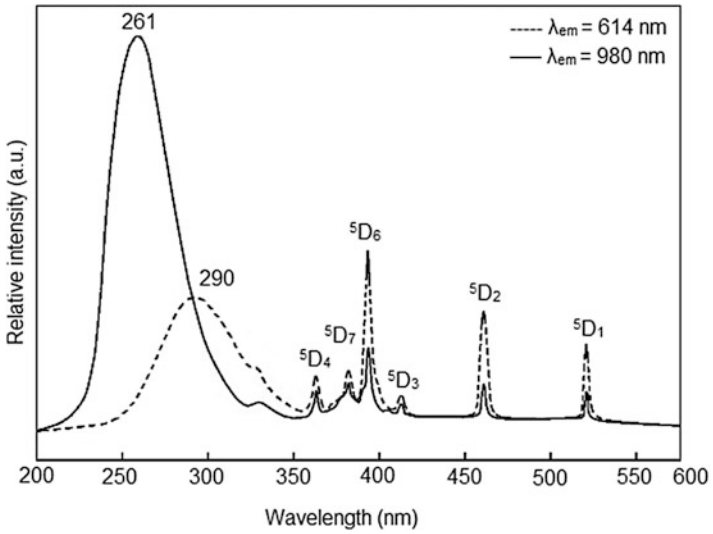

Fig. 11.8 Photoluminescent excitation spectra of Eu^{3+} emission monitored at 614 nm and Yb^{3+} emission monitored at 980 nm of [Eu $_{0.5}Yb_{0.5}$ $(sal)_3(phen)$] complex [82]

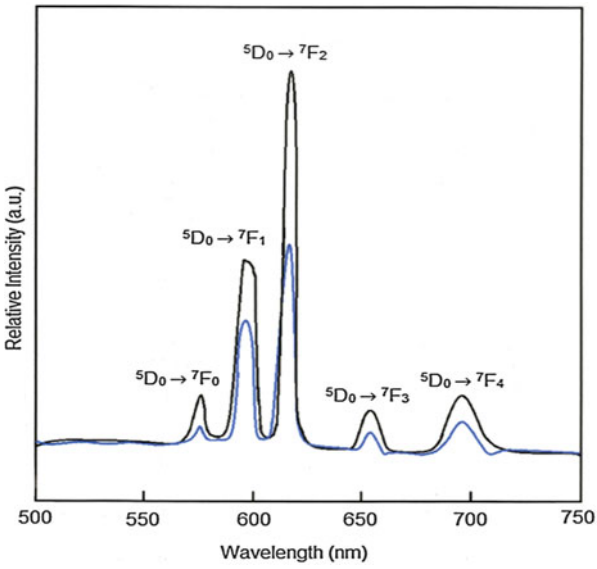

Fig. 11.9 Room temperature photoluminescent emission spectra of $[Eu(sal)_3(phen)]$ and $[Eu_{0.5}Yb_{0.5}(sal)_3(phen)]$ complexes excited at 384 nm [82]

wavelength. The quantum yield of lanthanide complexes involves several factors such as ligand to Ln(III) energy transfer, multiphonon-relaxation, energy back transfer, crossover to charge transfer states etc. [83] Also, there are several competing processes such as fluorescence of antenna (competes with intersystem crossing), quenching of triplet state by dissolved molecular oxygen in case of

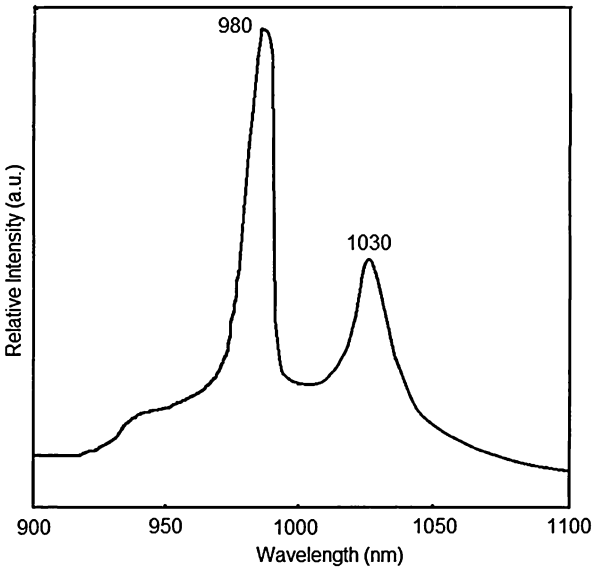

Fig. 11.10 Room temperature photoluminescent emission spectra of $[Yb(sal)_3(phen)]$ excited at 384 nm [82]

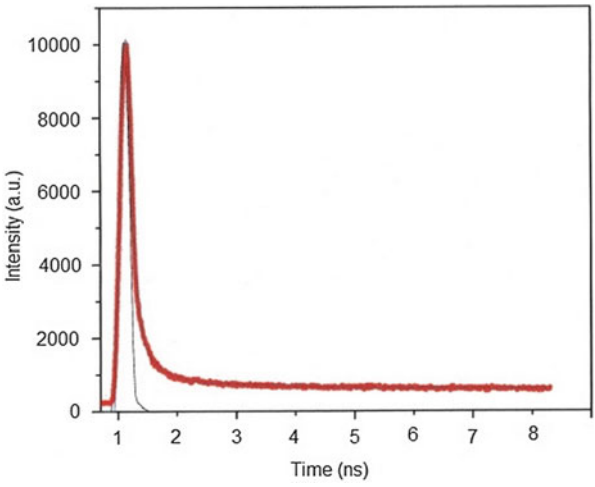

Fig. 11.11 Decay curve of Eu^{3+}, $^5D_0$ excited state (excitation wavelength: 384 nm; emission wavelength: 614 nm) of $[Eu_{0.5}Yb_{0.5}\ (sal)_3(phen)]$ complex [82]

NIR emitting ions (competes with energy transfer to the lanthanide ion) and the presence of solvent or water molecules which lowers the value of photoluminescence quantum yield. Hence, the overall quantum yield of sensitized emission (Φ_S) is the product of intersystem crossing quantum yield (Φ_{ISC}), the energy transfer quantum yield (Φ_{ET}) and the lanthanide luminescence quantum yield (Φ_{Lum})

$$\mathbf{\Phi_S = \Phi_{ISC} * \Phi_{ET} * \Phi_{Lum}} \tag{11.2}$$

The overall quantum yield of the lanthanide complexes with organic ligands can be calculated as:

$$\boldsymbol{\Phi}_{\boldsymbol{Ln}}^{\boldsymbol{L}} = \boldsymbol{\eta}_{\mathbf{sens}} \cdot \boldsymbol{\Phi}_{\boldsymbol{Ln}}^{\boldsymbol{Ln}} = \boldsymbol{\eta}_{\mathbf{sens}} \cdot \left(\frac{\boldsymbol{Krad}}{\boldsymbol{Kobs}} \right) = \boldsymbol{\eta}_{\mathbf{sens}} \cdot \left(\frac{\boldsymbol{\tau rad}}{\boldsymbol{\tau obs}} \right) \tag{11.3}$$

where $\Phi_{\mathrm{Ln}}^{\mathrm{L}}$ and $\boldsymbol{\Phi}_{\boldsymbol{Ln}}^{\boldsymbol{Ln}}$ represent the quantum yield resulting from indirect and direct excitation respectively and η_{sens} is the quantum efficiency with which the electromagnetic energy if transferred from the organic ligands to the lanthanide ion. K_{rad} is the radiative rate constant, K_{obs} is the sum total of rates of various deactivation processes and τ_{rad} is the radiative lifetime. The intrinsic quantum yield $\Phi_{\mathrm{Ln}}^{\mathrm{Ln}}$ can be calculated as:

$$\Phi_{\mathbf{Ln}}^{\mathbf{Ln}} = \mathbf{K_{rad}} / \left(\mathbf{K_{rad}} + \mathbf{K_{nr}} \right) \tag{11.4}$$

K_{nr} represents nonradiative rate constant which can be attributed to the back energy transfer to the sensitizer, quenching by matrix vibrations or by electron transfer mainly for the lanthanides having low reduction potential such as Eu(III) and Yb (III) ions [84]. The intrinsic quantum yield can be determined by two proposed mechanisms:

(a) The rapid diffusion enhanced resonance energy transfer after mixing the lanthanide complexes with a known quantum yield acceptor in solution and the efficiency of energy transfer between them can be calculated from both lifetime and intensity parameters.

(b) This mechanism is valid only for europium and relies on the fact that the intensity of purely magnetic dipolar transition $^5D_0 \rightarrow {}^7F_1$ transition is independent of the chemical environment of the lanthanide ion and the radiative lifetime can be calculated from the emission spectrum. The measurement of absolute quantum yield is a sophisticated task, it can be calculated by determination of relative quantum yield with that of standard sample of known absolute quantum yield. The absolute quantum yield of lanthanide complexes in solution can be calculated as:

$$\Phi_{\mathbf{S}} = \Phi_{\mathbf{ST}} \left(\mathbf{I_S} / \mathbf{I_{ST}} \right) \left(\mathbf{R} \boldsymbol{I}_{\boldsymbol{S}}^{\boldsymbol{2}} / \mathbf{R} \boldsymbol{I}_{\boldsymbol{ST}}^{\boldsymbol{2}} \right) \left(\mathbf{F_{ST}} / \mathbf{F_S} \right) \tag{11.5}$$

where Φ_{S} represents the absolute quantum yield of sample, Φ_{ST} is the absolute quantum yield of reference compound, $\mathrm{RI_S}$ and $\mathrm{RI_{ST}}$ are the refractive index of sample solvent and reference compound respectively and represents the fraction of light absorbed by reference and sample. The accurate determination of quantum yields includes a number of factors e.g. internal filter effects, self-quenching and reliability of the standard value [85]. The other important parameter termed as

luminescence lifetime can be defined as the time which an electron spent in excited state after excitation. It can be calculated as:

$$\boldsymbol{\tau_{obs}} = 1/\mathbf{K_{obs}} \tag{11.6}$$

The radiative rate (K_{rad}) and non-radiative rate (K_{nr}) can be calculated as:

$$\mathbf{K_{rad}} = \boldsymbol{\Phi}/\boldsymbol{\tau} \tag{11.7}$$

$$1/\boldsymbol{\tau} = \mathbf{K_{rad}} + \mathbf{K_{nr}} \tag{11.8}$$

The overall absorbance of the lanthanide complexes is increased by the direct and indirect attachment of the chromophores to the lanthanide ion. The energy transfer process from the ligand to the metal ion is explained by the Forster and Dexter mechanism for direct chromophore attachment, while in case of indirect attachment of chromophore, the energy transfer proceeds through Forster dipole-dipole mechanism. The separation between two chromophores can be accessible through the determination of energy transfer efficiency (η_{et}) and can be calculated as:

$$\boldsymbol{\eta_{et}} = 1 - (\boldsymbol{\tau_{obs}}/\boldsymbol{\tau}_0) = \mathbf{K}_0/\mathbf{K_{obs}} = 1/(1 + \mathbf{R_{DA}}/\mathbf{R}_0)^6 \tag{11.9}$$

where τ_{obs} and τ_0 are the lifetime of donor chromophore in presence and absence of acceptor chromophore respectively, K_0 and K_{obs} are the decay rates of acceptor without and with donor respectively. R_{DA} and R_0 are the distance between donor-acceptor and critical distance respectively. The critical distance depends on the quantum yield of donor Q_D without acceptor, refractive index *n* of the medium, the overlap integral J_{ov} between the emission spectrum of donor and absorption spectrum of acceptor and orientation factor κ having isotropic limit of 2/3 and can be calculated as:

$$\mathbf{R}_{06} = 8.75 \times 10^{-25}\left(\boldsymbol{\kappa}^2.\mathbf{J_{ov}}.\mathbf{Q_D}.\boldsymbol{n}^{-4}\right) \tag{11.10}$$

The Judd-Ofelt analysis is a useful technique to estimate the population of odd-parity electron transitions for Eu(III) complexes. The interaction parameters of the ligand fields can be calculated from the Judd-Ofelt parameter, Ω_λ. The parameter Ω_2 is more sensitive to the symmetry and sequence fields and for anti-symmetrical Eu(III) complexes Ω_2 is large for faster radiative rates. The experimental intensity parameters Ω_λ where $\lambda = 2$ and 4, can be determined from the emission spectrum of Eu(III) complexes based on $^5D_0 \rightarrow {}^7F_2$ and $^5D_0 \rightarrow {}^7F_4$ transitions where the $^5D_0 \rightarrow {}^7F_1$ magnetic dipole-allowed transition is taken as reference and can be estimated as:

$$\mathbf{A_{RAD}} = \left(4\mathbf{e}^2 2\boldsymbol{\omega}^3/3\hbar\mathbf{c}^3\right)\boldsymbol{\chi}\sum\nolimits_\lambda \boldsymbol{\Omega}_\lambda < {}^7\mathbf{F_J}\left|\mathbf{U}^{(\lambda)}\right|{}^5\mathbf{D}_0 >^2 .(1/2\mathbf{J}+1) \tag{11.11}$$

A_{RAD} is the correspondent coefficient of spontaneous emission, e is the charge on electron, ω is the angular frequency of the transition, ħ is the Planck's constant

over 2л, c is velocity of light and χ is the Lorentz local field correction term which is given by $n(n^2+2)^2/9$ with a refraction index $n = 1.43$ and $< {}^7F_J \mid U^{(\lambda)} \mid {}^5D_0 >^2$ are the squared reduced matrix elements with values of 0.0032 and 0.0023 for $J = 2$ and 4 respectively. The Ω_6 parameter is difficult to determine as ${}^5D_0 \rightarrow {}^7F_6$ transition cannot be experimentally detected in most of Eu(III) complexes.

11.4 Lanthanide Doped Upconversion Nanoparticles

Lanthanide–doped upconversion nanoparticles (UCNPs) are mainly composed of three key components: a host matrix, sensitizer and activator. Generally, these UCNPs are fabricated by doping the trivalent lanthanides which have metastable excited states into an inorganic crystalline host lattice that can host these dopant ions. In case of lanthanide doped UCNPs, the sensitizer absorbs photons at 980 nm due to which it is excited to the higher energy state. The activator ions now obtain energy from the sensitizers to reach their corresponding excited states and show emission at short wavelengths (Fig. 11.12).

The selection of the host materials is important as it determines the lattice between the dopant ions, relative spatial position, coordination numbers and the type of anions surrounding the dopant. Several conditions need to be fulfilled while choosing the host lattice as reviewed by Wang and Liu (2009) [86, 87] and Ong *et. al*. (2010) [88] are (i) close lattice matches to dopant ions; (ii) low phonon vibration energies and (iii) good chemical stability. The host lattice must be able to accommodate the lanthanide dopant ions as it largely affects the luminescence output and emission intensity ratios of different transitions. The phonon energy of the host lattice must be low to ensure homogeneous doping and minimizing the lattice stress and non-radiative energy loss. The fluoride compounds serve as best host lattices due to their low phonon energy (350 cm^{-1}) and high chemical stability. These compounds are LaF_4, YF_4, $NaYF_4$ and $BaYF_4$ which are widely used as optimal host materials. The longer lifetimes are observed for the excited states of fluorides lattices due to the low phonon energies of the crystal lattice [89]. The lattice impurities increase the multi-phonon relaxation rates between the metastable states, thereby reducing the overall visible emission intensity. The halogenides also have small radiative losses but these materials have low chemical stability. The oxides have high chemical stability but their phonon energy is high (>500 cm^{-1}) due to stretching vibration of host lattice. Therefore fluorides prove to be ideal host candidates for the green and blue upconversion phosphors.

The upconverting luminescence efficiency depends upon nature of absorbers/emitters and the doping concentration of absorbers/emitters. The luminescence efficiency is highest when the doping concentration of absorbers/emitters shows well matching energy level. The improper absorber/emitter doping concentration ratio results concentration related cross-relaxation quenching or disables energy transfer. Among the lanthanide ions, Yb^{3+} ions are frequently used as absorbers due to its simple energy levels ${}^2F_{5/2}$ and ${}^2F_{7/2}$ and high absorption coefficient at 980 nm

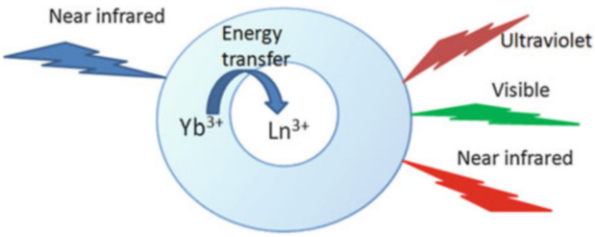

Fig. 11.12 The energy transfer process in up-conversion nanoparticles

and are used in relatively high doping ratios (20–30 %) [90]. Some other lanthanide ions like Er^{3+}, Tm^{3+} and Ho^{3+} have ladder-like energy levels and are often used as activators with low doping concentrations. The other lanthanide ions (Y^{3+}, La^{3+}, Gd^{3+}, Sc^{3+}), transition metal ions (Zr^{4+}, Ti^{4+}) and alkaline earth ions (Ca^{2+}, Sr^{2+}, Ba^{2+}) are also suitable ions that can be used. The most practical hosts are the halides ($NaYF_4$, YF_3, LaF_3), oxides (Y_2O_3, ZrO_2) and oxysulphides (Y_2O_2S, La_2O_2S) due to their low phonon-energy lattice. These hosts reduce multi-phonon relaxation and increase the lifetime of the intermediate states involved in upconversion process [91]. Thus to overcome the limitations of conventional fluoroprobes the lanthanide doped hexagonal phase $NaYF_4$ upconverting materials are appropriate substituents due to their superior upconverting properties.

The nano lanthanide doped oxide hosts are extensively reported with regard to Y_2O_3 as an important host material. It has broad transparency range (0.2–8 nm) with a band gap of 5.6 eV, high refractive index, better thermal conductivity and low phonon energy that makes it an attractive choice as the host material. The mostly used lanthanide host-dopant systems are listed in Table 11.2.

11.4.1 Mechanism of Upconversion

The conventional fluorophores exhibit the phenomenon of downconversion, i.e. higher energy photons are absorbed while lower energy ones are emitted due to energy loss (IEL). Compared with downconversion, upconversion is a process that causes the emission of higher energy photons through sequential absorption of lower energy photons. The mechanism of upconversion process has been extensively studied and is generally divided into three steps: excited state absorption (ESA), energy transfer upconversion (ETU) and photon avalanche (PA). In comparison with the other two processes, ETU has been widely employed to obtain high upconversion efficiency (emission density versus NIR excitation power), involving the absorption of a pump phonon of the same energy by each of the two neighboring ions. A subsequent non-radiative energy transfer promotes one of the ions to an upper energy level (EL2) while the other ion relaxes back to the ground state (GS). The relaxation from EL2 results in the emission of higher energy photons [98] (Fig. 11.13).

Table 11.2 Representative UCNPs with different host-dopant systems, excitation wavelengths and emission peaks [92–97]

Dopant ions			Major emissions (nm)		
Host lattice	Sensitizer	Activator	Blue	Green	Red
$NaYF_4$	Yb	Er		518, 537	652
	Yb	Er		540	660
	Yb	Er		510–530	635–675
	Yb	Er		521,539	651
LaF_3	Yb	Tm	475		
	Yb	Er		520, 545	659
CaF_2	Yb	Er		524	654
Y_2O_3	Yb	Er		550	660
Lu_2O_3	Yb	Er, Tm	490	540	662
$LuPO_4$	Yb	Tm	475		649

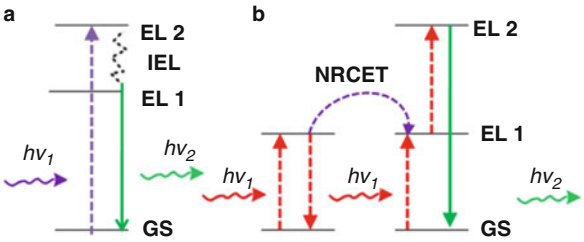

Fig. 11.13 Illustration of (**a**) downconversion and (**b**) energy transfer upconversion mechanism. *IEL* internal energy loss, *GS* ground state, *EL* energy level, *NRET* nonradiative energy transfer, *hvl* incident light, *hv2* emission light [98]

11.4.2 Enhancing the Up Conversion Efficiency

The lanthanide–doped nanoparticles have great potential as lasers, phosphors and recently biolabels as well. The possibility to enhance the up-conversion luminescence has always been an interesting research topic. These nanoluminophores act as efficient biolabels when compared to organic dyes and quantum dots due to their excellent photostability, efficient near infrared to visible and long luminescence lifetimes suitable for time delayed detection. There is a need to enhance the up-conversion efficiency as these UCNPs suffer from low brightness when compared to conventional biolabels. There are certain ways to modify the upconversion efficiency which includes the dopant concentration, modifying the local chemical and structural environment, controlling the distribution of active ions in host material, varying the composition, structure and morphology of the up-converting nanoparticles. These factors reduce the quenching effect, enhance the absorption of NIR radiation or improve the sensitizer to activator energy transfer.

11.4.2.1 Concentration of Optically Active Ions

The up-conversion quantum yield can be enhanced by increasing the concentration of optically active ions within a single nanoparticle as the upconversion in singly doped NPs is very weak, therefore it is necessary to co-doping the activator ions with the sensitizer ions. The enhanced up-conversion in doubly doped material was first studied by F. Auzel in 1966 [99]. Yb^{3+} ion is most frequently used sensitizing lanthanide ion due to its simple energy levels, large absorption cross section at 940–990 nm in NIR region and large energy gap (10,000 cm^{-1}) and long luminescence lifetimes (1 ms). Yb^{3+} is usually chosen as it absorbes in NIR region and further capable of transferring its energy to the activator ions such as Tm^{3+}, Er^{3+} in the energy transfer up-conversion process which requires a single activator ions surrounded by atleast two or three Yb^{3+} ions.

The increase in the activator ions concentration results in the decrease in the effective distance between the ions and when the energy levels are quasi-resonant, the excited ions become non-radiatively depopulated. The concentration quenching manifests itself in shortening the luminescence lifetimes as well as in decreasing the effective luminescence quantum yield enhancement despite the increase in luminescence centres. Therefore the concentration of the activator ions must be carefully optimized. The NIR PL emission from the ultrasmall $NaYF_4$: 2 % Tm^{3+} nanocrystals to be 3.6 times more intense than the one from conventional 25–30 nm sized $NaYF_4$: 20 % Yb^{3+} / Tm^{3+} nanocrystals. These Yb^{3+} / Tm^{3+} doped UCNPs are particularly attractive due to highly efficient NIR-to-NIR conversion i.e. 980 nm excitation to 800 nm up conversion emission [100].

11.4.2.2 Selection of Host Material

The up conversion efficiency can be enhanced by the proper selection of the host material for lanthanide ion dopants. The low energy phonons cause low non-radiative and multiphonon losses and increase the luminescence lifetimes. Different hosts such as chlorides, bromides and iodides with phonon energies of ~144, 172 and 260 cm^{-1} and low multiphonon relaxation rates are suitable for up-conversion process as compared to fluorides and oxides [101]. Concluding, we can say that the selection of the host material is a balance between phonon properties and excitation spectra intensity which makes the host material appropriate for energy up-conversion in lanthanide doped materials.

11.4.2.3 Impurities in Host Matrix

The up-conversion efficiency can be enhanced by co-doping passive or active impurities in an efficient way. In case of passive impurities, the doping ions induce distortions to the local symmetry around activators or dissociate the lanthanide

clusters in the nanocrystals and leads to increase in the up-conversion efficiency. These impurities do not participate in energy transfer within the matrix. On the other hand, the active impurities modify the energy transfer rates within the system and enhance the up-conversion efficiency. The enhancement of up-conversion efficiency in singly Er^{3+} -doped $YAlO_3$ phosphor by exchanging 40 % of Y^{3+} ions by larger Gd^{3+} ions (0.1159, 0.1193 nm) resulting in expanding the host lattice and distorting the local symmetry as studied by Li et.al [102]. The co-doping of β-$NaGdF_4$: Yb^{3+} /Er^{3+} nanoparticles with different amount of Li^+ ions also showed a higher up conversion enhancement as studied by Cheng et.al [103]. The green and red up-conversion emission yield intensities of the nanoparticles co-doped with 7 mol % Li^+ ions were enhanced 47 and 23 times respectively. The alkali ions also have an impact on the structure and spectral properties of up-converting fluoride nanocrystals. The phase, size, shape and stability of the Yb/Er co-doped $NaYF_4$ also get affected by the Li^+ and K^+ content, the green to blue ratio varied in the range ~2–6.5 and ~0.7–1.7 respectively and rose to 20–80 %. The passive impurities affect activator distribution within the UCNP, the active impurities also play a critical role in the energy transfer. This approach leads to the modification of energy distribution as well as the interaction between respective excited energy levels of the co-doping lanthanides. The improvement in the up-conversion quantum yield by the co-doping of Tm^{3+} and Er^{3+} activators with the Yb^{3+} sensitizers serves as an important example.

11.5 Synthesis of Lanthanide Doped UCNPs

The various chemical approaches for the synthesis of Ln-doped UCNPs have been studied by Wang and Liu in 2009 [104], these methods such as co-precipitation, thermal decomposition, sol-gel method and hydro thermal method are discussed as:

11.5.1 Co-precipitation Method

The co-precipitation method is simple as it does not require costly set up, complex procedures and severe reaction conditions. In this method, the nanoparticle growth can be controlled and stabilized by adding capping ligands such as polyvinylpyrrolidone (PVP), polyethylenimine (PEI) and ethylene diaminetetraacetic acid (EDTA) into the solvent. This method generally yields cubic phase $NaYF_4$: Yb, Er which is not an efficient up-convertor, subsequent calcinations at high temperatures results in sharpened crystal structure or partial phase transfer to hexagonal – phase $NaYF_4$: Yb, Er which has higher upconversion efficiency as studied by Yi et. al [105].

11.5.2 Thermal Decomposition Method

This method involves dissolving of organic precursors in high boiling point solvents (e.g. oleic acid (OA), oleylamine (OM), octadecene(ODE) for the synthesis of highly monodispersed UCNPs. The rare earth trifluoroacetates are thermolyzed in the presence of high boiling point solvents at a temperature usually exceeding 300 °C. Mai et.al [106]. synthesized Er^{3+}, Yb^{3+} and Tm^{3+}, Yb^{3+} doped monodispersed cubic-phase and hexagonal-phase $NaYF_4$ nanocrystals by the thermal decomposition of trifluoroacetate precursors in OA/OM/ODE solvents and OA/ODE solvents respectively and also synthesized $NaYF_4$ based UCNPs with different luminescent properties with similar synthetic methods. Yi and Chow [107] obtained hexagonal-phase $NaYF_4$:Yb, Er and $NaYF_4$:Yb, Tm nanoparticles with an average particle size of 10.5 nm by decomposing the precursors of Na (CF_3COO), $Y(CF_3COO)_3$, $Yb(CF_3COO)_3$ and $Er(CF_3COO)_3/Tm(CF_3COO)_3$ in OM solvent at 300 °C with much higher up-conversion fluorescence intensity. This method however, has some disadvantages such as use of expensive and air-sensitive metal precursors and the generation of toxic by-products.

11.5.3 Sol Gel Method

The sol-gel method is mainly based on the hydrolysis and polycondensation of metal alkoxides or metal acetate precursors to form extended networks with an oxide skeleton. Li et.al [108]. studied the preparation of metal oxide based Ln-doped UCNPs such as $YV0_4$:Yb, Er, $Lu_3Ga_5O_{12}$: Er, $BaTiO_3$: Er and ZrO_2:Er by the sol-gel method. Though this method is good for the synthesis of various Ln-doped UCNPs, however there are certain limitations such as particle size and particle aggregation may occur when dispersed in aqueous solution. Some post treatments are often needed to improve the crystalline phase purity for enhanced luminescence efficiency.

11.5.4 Hydrothermal Method

The synthesis of highly crystalline nanocrystals with tunable size, morphology, optical and magnetic properties via controlled reaction temperature, time, concentration, pH and precursors etc can be done by hydrothermal method. This method improves the solubility of solids under hydrothermal conditions, which accelerates the reactions between solids. The advantage of this method lies in the fact that it requires “one-pot process” with heat resistant polymer (PEI, PVP) added to the solvent. Wang et.al [109]. studied the preparation of uniform-sized nanoparticles with appropriate surface modification which were obtained by single reaction

process. The only limitation with the hydrothermal method is the difficulty in observing the nanocrystals growth process.

11.6 Conclusion

Recently the luminescent lanthanide complexes are receiving the attention of scientific fraternity due to their high luminous lifetimes and extremely sharp emission bands arising from the electronic transitions between the 4f energy levels. The lanthanide complexes are widely used in many technologically interesting fields such as photoluminescent materials in display devices, fluorescence probes and labels in biological systems. In order to design the efficient luminescent fluorophores, it is necessary to understand the electronic and spectroscopic properties of rare earth elements, basic principles of photoluminescence which includes the basic concepts of antenna effect, coordination features of Ln^{3+} ions, radiative lifetime and photoluminescence quantum yield of lanthanide complexes. Apart from the luminescent lanthanide complexes, the lanthanide up-converting nanoparticles possess great potential as novel fluorophores for biological applications. These exhibit unique fluorescent property providing tremendous applications which have enormous advantages over conventional fluorophores. This review insights into the main aspects related to design of luminescent lanthanide complexes and lanthanide up-converting nanoparticles and also gives an overview of our recent work on photoluminescent properties of lanthanide complexes with nitrogen donor and oxygen donor ligands. The synthesis and photoluminescence properties of europium and ytterbium complexes with 2-aminopyridine, 1,10-phenanthroline, dipicolinic acid, α-picolinic acid, salicylic acid and 2-hydroxypyridine have been reported. The prepared complexes can act as good candidates for fluorescence probes and optoelectronic devices.

Acknowledgement The authors acknowledge Guru Gobind Singh Indraprastha University, New Delhi for providing financial support in the form of Indraprastha research fellowship (IPRF) for research work. Also, the authors are thankful to Ms. Shruti Peshoria for her contribution in preparation of the manuscript.

References

1. Di Bernardo P, Melchior A, Tolazzi M, Zanonato PL (2012) Thermodynamics of lanthanide (III) complexation in non-aqueous solvents. Coord Chem Rev 256(1–2):328–351
2. Bünzli J-CG, Chauvin A-S, Kim HK, Deiters E, Eliseeva SV (2010) Lanthanide luminescence efficiency in eight- and nine-coordinate complexes: role of the radiative lifetime. Coord Chem Rev 254(21–22):2623–2633

3. Li H-Y, Wu J, Huang W, Zhou Y-H, Li H-R, Zheng Y-X, Zuo J-L (2009) Synthesis and photoluminescent properties of five homodinuclear lanthanide (Ln^{3+}=Eu^{3+}, Sm^{3+}, Er^{3+}, Yb^{3+}, Pr^{3+}) complexes. J Photochem Photobiol A 208(2–3):110–116
4. Sengar RS, Nigam A, Geib SJ, Wiener EC (2009) Syntheses and crystal structures of gadolinium and europium complexes of AAZTA analogues. Polyhedron 28(8):1525–1531
5. Pietraszkiewicz O, Pietraszkiewicz M, Karpiuk J, Jesień M (2009) Eu(III) complexes involving 1,3,5-triazine diphosphine oxides. J Rare Earths 27(4):584–587
6. Vicentini G, Zinner LB, Zukerman-Schpector J, Zinner K (2000) Luminescence and structure of europium compounds. Coord Chem Rev 196(1):353–382
7. Eliseeva SV, Bunzli J-CG (2010) Lanthanide luminescence for functional materials and bio-sciences. Chem Soc Rev 39(1):189–227
8. Montgomery CP, Murray BS, New EJ, Pal R, Parker D (2009) Cell-penetrating metal complex optical probes: targeted and responsive systems based on lanthanide luminescence. Acc Chem Res 42(7):925–937
9. Tsukube H, Shinoda S (2002) Lanthanide complexes in molecular recognition and chirality sensing of biological substrates. Chem Rev 102(6):2389–2404
10. Pandya S, Yu J, Parker D (2006) Engineering emissive europium and terbium complexes for molecular imaging and sensing. Dalton Trans 23:2757–2766
11. Duke RM, Veale EB, Pfeffer FM, Kruger PE, Gunnlaugsson T (2010) Colorimetric and fluorescent anion sensors: an overview of recent developments in the use of 1,8-naphthalimide-based chemosensors. Chem Soc Rev 39(10):3936–3953
12. dos Santos CMG, Harte AJ, Quinn SJ, Gunnlaugsson T (2008) Recent developments in the field of supramolecular lanthanide luminescent sensors and self-assemblies. Coord Chem Rev 252(23–24):2512–2527
13. Shinoda S, Tsukube H (2011) Luminescent lanthanide complexes as analytical tools in anion sensing, pH indication and protein recognition. Analyst 136(3):431–435
14. Tsukube H, Yano K, Shinoda S (2009) Near-infrared luminescence sensing of glutamic acid, aspartic acid, and their dipeptides with tris(β-diketonato)lanthanide probes. Helv Chim Acta 92(11):2488–2496
15. Bünzli J-CG (2006) Benefiting from the unique properties of lanthanide ions. Acc Chem Res 39(1):53–61
16. Evans RC, Douglas P, Winscom CJ (2006) Coordination complexes exhibiting room-temperature phosphorescence: evaluation of their suitability as triplet emitters in organic light emitting diodes. Coord Chem Rev 250(15–16):2093–2126
17. Yongliang Z, Fengying Z, Qiang L, Deqing G (2006) Synthesis, characterization and fluorescence properties of europium, terbium complexes with biphenyl-4-carboxylic acid and o-phenanthroline. J. Rare Earths 24(1, Supplement 1):18–22
18. Bunzli J-CG, Piguet C (2005) Taking advantage of luminescent lanthanide ions. Chem Soc Rev 34(12):1048–1077
19. Kido J, Okamoto Y (2002) Organo lanthanide metal complexes for electroluminescent materials. Chem Rev 102(6):2357–2368
20. Faulkner S, Pope SJA, Burton-Pye BP (2005) Lanthanide complexes for luminescence imaging applications. Appl Spectrosc Rev 40(1):1–31
21. Whan RE, Crosby GA (1962) Luminescence studies of rare earth complexes: benzoylacetonate and dibenzoylmethide chelates. J Mol Spectrosc 8(1–6):315–327
22. Crosby GA, Whan RE, Alire RM (1961) Intramolecular energy transfer in rare earth chelates. Role of the triplet state. J Chem Phys 34(3):743–748
23. Martell AE, Hancock RD, Motekaitis RJ (1994) Factors affecting stabilities of chelate, macrocyclic and macrobicyclic complexes in solution. Coord Chem Rev 133:39–65
24. Bünzli J-CG, Piguet C (2002) Lanthanide-containing molecular and supramolecular polymetallic functional assemblies. Chem Rev 102(6):1897–1928
25. Piguet C, Bunzli J-CG (1999) Mono- and polymetallic lanthanide-containing functional assemblies: a field between tradition and novelty. Chem Soc Rev 28(6):347–358

26. Kuriki K, Koike Y, Okamoto Y (2002) Plastic optical fiber lasers and amplifiers containing lanthanide complexes. Chem Rev 102(6):2347–2356
27. Yanagida S, Hasegawa Y, Murakoshi K, Wada Y, Nakashima N, Yamanaka T (1998) Strategies for enhancing photoluminescence of Nd3+ in liquid media. Coord Chem Rev 171:461–480
28. Hasegawa Y, Wada Y, Yanagida S (2004) Strategies for the design of luminescent lanthanide (III) complexes and their photonic applications. J Photochem Photobiol C 5(3):183–202
29. Sivakumar S, van Veggel FCJM, Raudsepp M (2005) Bright white light through Up-conversion of a single NIR source from sol–gel-derived thin film made with Ln3+−doped LaF3 nanoparticles. J Am Chem Soc 127(36):12464–12465
30. Werts MHV, Jukes RTF, Verhoeven JW (2002) The emission spectrum and the radiative lifetime of Eu3+ in luminescent lanthanide complexes. Phys Chem Chem Phys 4 (9):1542–1548
31. Tamaki S, Hasegawa Y, Yajima H (2013) Factors influencing the luminescence intensity of europium(III) complexes prepared via synergistic extraction. Talanta 105:262–266
32. Pandya S, Yu J, Parker D (2006) Engineering emissive europium and terbium complexes for molecular imaging and sensing. Dalton Trans 23:2757–2766
33. Johnsson N, Johnsson K (2007) Chemical tools for biomolecular imaging. ACS Chem Biol 2 (1):31–38
34. Clapp AR, Medintz IL, Mattoussi H (2006) Förster resonance energy transfer investigations using quantum-dot fluorophores. ChemPhysChem 7(1):47–57
35. Bazin H, Trinquet E, Mathis G (2002) Time resolved amplification of cryptate emission: a versatile technology to trace biomolecular interactions. Rev Mol Biotechnol 82(3):233–250
36. Shiraishi Y, Furubayashi Y, Nishimura G, Hirai T (2007) Sensitized luminescence properties of dinuclear lanthanide macrocyclic complexes bearing a benzophenone antenna. J Lumin 127(2):623–632
37. Werts MHV, Woudenberg RH, Emmerink PG, van Gassel R, Hofstraat JW, Verhoeven JW (2000) A near-infrared luminescent label based on YbIII ions and its application in a fluoroimmunoassay. Angew Chem Int Ed 39(24):4542–4544
38. Zhang J, Badger PD, Geib SJ, Petoud S (2005) Sensitization of near-infrared-emitting lanthanide cations in solution by tropolonate ligands. Angew Chem Int Ed 44(17):2508–2512
39. Comby S, Gumy F, Bünzli J-CG, Saraidarov T, Reisfeld R (2006) Luminescent properties of an Yb podate in sol–gel silica films, solution, and solid state. Chem Phys Lett 432 (1–3):128–132
40. Comby S, Imbert D, Vandevyver C, Bünzli J-CG (2007) A novel strategy for the design of 8-hydroxyquinolinate-based lanthanide bioprobes that emit in the near infrared range. Chem Eur J 13(3):936–944
41. Bassett AP, Van Deun R, Nockemann P, Glover PB, Kariuki BM, Van Hecke K, Van Meervelt L, Pikramenou Z (2005) Long-lived near-infrared luminescent lanthanide complexes of imidodiphosphinate "shell" ligands. Inorg Chem 44(18):6140–6142
42. Imbert D, Cantuel M, Bünzli J-CG, Bernardinelli G, Piguet C (2003) Extending lifetimes of lanthanide-based near-infrared emitters (Nd, Yb) in the millisecond range through Cr(III) sensitization in discrete bimetallic edifices. J Am Chem Soc 125(51):15698–15699
43. Torelli S, Imbert D, Cantuel M, Bernardinelli G, Delahaye S, Hauser A, Bünzli J-CG, Piguet C (2005) Tuning the decay time of lanthanide-based near infrared luminescence from micro- to milliseconds through d→f energy transfer in discrete heterobimetallic complexes. Chem Eur J 11(11):3228–3242
44. Picot A, Malvolti F, Le Guennic B, Baldeck PL, Williams JAG, Andraud C, Maury O (2007) Two-photon antenna effect induced in octupolar europium complexes. Inorg Chem 46 (7):2659–2665
45. Fu L-M, Wen X-F, Ai X-C, Sun Y, Wu Y-S, Zhang J-P, Wang Y (2005) Efficient two-photon-sensitized luminescence of a europium(III) complex. Angew Chem Int Ed 44 (5):747–750

46. Manning HC, Goebel T, Thompson RC, Price RR, Lee H, Bornhop DJ (2004) Targeted molecular imaging agents for cellular-scale bimodal imaging. Bioconjug Chem 15 (6):1488–1495
47. Alzakhem N, Bischof C, Seitz M (2012) Dependence of the photophysical properties on the number of 2,2′-bipyridine units in a series of luminescent europium and terbium cryptates. Inorg Chem 51(17):9343–9349
48. Bornhop DJ, Hubbard DS, Houlne MP, Adair C, Kiefer GE, Pence BC, Morgan DL (1999) Fluorescent tissue site-selective lanthanide chelate, Tb-PCTMB for enhanced imaging of cancer. Anal Chem 71(14):2607–2615
49. Hanaoka K, Kikuchi K, Kojima H, Urano Y, Nagano T (2003) Selective detection of zinc ions with novel luminescent lanthanide probes. Angew Chem Int Ed 42(26):2996–2999
50. Hanaoka K, Kikuchi K, Kojima H, Urano Y, Nagano T (2004) Development of a zinc Ion-selective luminescent lanthanide chemosensor for biological applications. J Am Chem Soc 126(39):12470–12476
51. Parker D (2000) Luminescent lanthanide sensors for pH, pO2 and selected anions. Coord Chem Rev 205(1):109–130
52. Pal R, Parker D (2007) A single component ratiometric pH probe with long wavelength excitation of europium emission. Chem Commun 5:474–476
53. Song B, Wang G, Tan M, Yuan J (2006) A europium(III) complex as an efficient singlet oxygen luminescence probe. J Am Chem Soc 128(41):13442–13450
54. Bencini A, Lippolis V (2010) 1,10-phenanthroline: a versatile building block for the construction of ligands for various purposes. Coord Chem Rev 254(17–18):2096–2180
55. Stan CS, Rosca I, Sutiman D, Secula MS (2012) Highly luminescent europium and terbium complexes based on succinimide and N-hydroxysuccinimide. J Rare Earths 30(5):401–407
56. Pérez-Mayoral E, Soler-Padrós J, Negri V, Cerdán S, Ballesteros P (2007) Synthetic approaches to heterocyclic ligands for Gd-based MRI contrast agents. Molecules 12 (8):1771–1795
57. Strasser A, Vogler A (2004) Phosphorescence of gadolinium(III) chelates under ambient conditions. Inorg Chim Acta 357(8):2345–2348
58. Yuan W, Cui Y, Shi R, Tao D, Wang Y, Zhang W, Chen J, Sun L, Liu S, Xu Y (2011) Study on fluorescence properties of rare earth complexes influenced by steric effect. J Rare Earths 29(11):1013–1017
59. Wang Q-M, Yan B (2004) From molecules to materials: a new way to construct luminescent chemical bonded hybrid systems based with ternary lanthanide complexes of 1,10-phenanthroline. Inorg Chem Commun 7(10):1124–1127
60. Wang D, Pi Y, Zheng C, Fan L, Hu Y, Wei X (2013) Preparation and photoluminescence of some europium (III) ternary complexes with β-diketone and nitrogen heterocyclic ligands. J Alloys Compd 574:54–58
61. Sharma G, Narula AK (2015) Synthesis of Eu(III) complexes with 2-aminopyridine and 1,10-phenanthroline: structural, optical, thermal and morphological studies. Sens Actuators B Chem 215:584–591
62. Lin M, Wang X, Tang Q, Ling Q (2013) Luminescence properties of polymers containing europium complexes with 4-tert-butylbenzoic acid. J Rare Earths 31(10):950–956
63. Zhuravlev KP, Tsaryuk VI, Pekareva IS, Sokolnicki J, Klemenkova ZS (2011) Europium and terbium ortho-, meta-, and para-methoxybenzoates: structural peculiarities, luminescence, and energy transfer. J Photochem Photobiol A 219(1):139–147
64. Räsänen M, Takalo H, Rosenberg J, Mäkelä J, Haapakka K, Kankare J (2014) Study on photophysical properties of Eu(III) complexes with aromatic β-diketones – role of charge transfer states in the energy migration. J Lumin 146:211–217
65. Lahoud MG, Marques LF, da Silva PB, de Jesus CAS, da Silva CCP, Ellena J, Freitas RS, Davolos MR, Frem RCG (2013) Synthesis, crystal structure and photoluminescence of a binuclear complex of europium(III) containing 3,5-dicarboxypyrazolate and succinate. Polyhedron 54:1–7

66. Zucchi G, Maury O, Thuéry P, Ephritikhine M (2008) Structural diversity in neodymium bipyrimidine compounds with near infrared luminescence: from mono- and binuclear complexes to metal-organic frameworks. Inorg Chem 47(22):10398–10406
67. Armelao L, Quici S, Barigelletti F, Accorsi G, Bottaro G, Cavazzini M, Tondello E (2010) Design of luminescent lanthanide complexes: from molecules to highly efficient photo-emitting materials. Coord Chem Rev 254(5–6):487–505
68. de Sá GF, Malta OL, de Mello Donegá C, Simas AM, Longo RL, Santa-Cruz PA, da Silva Jr EF (2000) Spectroscopic properties and design of highly luminescent lanthanide coordination complexes. Coord Chem Rev 196(1):165–195
69. Azab HA, Duerkop A, Anwar ZM, Hussein BHM, Rizk MA, Amin T (2013) Luminescence recognition of different organophosphorus pesticides by the luminescent Eu(III)–pyridine-2,6-dicarboxylic acid probe. Anal Chim Acta 759:81–91
70. Zheng H, Gao D, Fu Z, Wang E, Lei Y, Tuan Y, Cui M (2011) Fluorescence enhancement of Ln3+ doped nanoparticles. J Lumin 131(3):423–428
71. Zhang L, An Y, Ahmad W, Zhou Y, Shi Z, Zheng X (2013) A new quaternary luminescence enhancement system of Eu–N-(3-methoxysalicylidene)-2-aminopyridine–1,10-phenanthroline–Zn and its application in determining trace amounts of Eu3+ and Zn2+. J Photochem Photobiol A 252:167–173
72. Sharma G, Narula A (2015) Synthesis and optoelectronic properties of three Eu(III)-dipicolinate complexes based on α-picolinic acid, 2-aminopyridine and 2-hydroxypyridine as secondary ligands. J Mater Sci Mater Electron 26(2):1009–1017
73. Yue Q, Yang J, Li G-H, Li G-D, Xu W, Chen J-S, Wang S-N (2005) Three-dimensional 3d–4f heterometallic coordination polymers: synthesis, structures, and magnetic properties. Inorg Chem 44(15):5241–5246
74. Bünzli J-CG (2010) Lanthanide luminescence for biomedical analyses and imaging. Chem Rev 110(5):2729–2755
75. Tsukube H, Shinoda S (2002) Lanthanide complexes in molecular recognition and chirality sensing of biological substrates. Chem Rev 102(6):2389–2404
76. de Lill DT, de Bettencourt-Dias A, Cahill CL (2007) Exploring lanthanide luminescence in metal-organic frameworks: synthesis, structure, and guest-sensitized luminescence of a mixed europium/terbium-adipate framework and a terbium-adipate framework. Inorg Chem 46(10):3960–3965
77. Ma D, Wang W, Li Y, Li J, Daiguebonne C, Calvez G, Guillou O (2010) In situ 2,5-pyrazinedicarboxylate and oxalate ligands synthesis leading to a microporous europium-organic framework capable of selective sensing of small molecules. CrystEngComm 12(12):4372–4377
78. Huang J, Xu Y, Chen X, Xu D, Xu Y, He Q (2012) Synthesis, characterization and properties of some rare earth complexes with 2,6-pyridine dicarboxylic acid and α-Picolinic acid. J Rare Earths 30(6):586–591
79. Mistri S, Zangrando E, Manna SC (2013) Cu(II) complexes of pyridine-2,6-dicarboxylate and N-donor neutral ligands: synthesis, crystal structure, thermal behavior, DFT calculation and effect of aromatic compounds on their fluorescence. Inorg Chim Acta 405:331–338
80. Jose SP, Mohan S (2006) Vibrational spectra and normal co-ordinate analysis of 2-aminopyridine and 2-amino picoline. Spectrochim Acta A Mol Biomol Spectrosc 64 (1):240–245
81. Dwivedi Y, Rai A, Rai SB (2009) Energy transfer in Er:Eu:Yb co-doped tellurite glasses: Yb as enhancer and quencher. J Lumin 129(6):629–633
82. Sharma G, Narula A (2015) Eu3+, Yb3+ and Eu3+−Yb3+ complexes with salicylic acid and 1,10-phenanthroline: synthesis, photoluminescent properties and energy transfer. J Fluoresc 25(2):355–360
83. Łyszczek R, Mazur L (2012) Polynuclear complexes constructed by lanthanides and pyridine-3,5-dicarboxylate ligand: Structures, thermal and luminescent properties. Polyhedron 41 (1):7–19

84. Beeby A, Clarkson IM, Dickins RS, Faulkner S, Parker D, Royle L, de Sousa AS, Gareth Williams JA, Woods M (1999) Non-radiative deactivation of the excited states of europium, terbium and ytterbium complexes by proximate energy-matched OH, NH and CH oscillators: an improved luminescence method for establishing solution hydration states. J Chem Soc Perkin Trans 2(3):493–504
85. Dwivedi Y, Thakur SN, Rai SB (2007) Study of frequency upconversion in Yb3+/Eu3+ by cooperative energy transfer in oxyfluoroborate glass matrix. Appl Phys B 89(1):45–51
86. Yang CH, Yang GF, Pan YX, Zhang QY (2009) Synthesis and spectroscopic properties of GdAl3(BO3)4 poly-crystals codoped with Yb3+ and Eu3+. J Fluoresc 19(1):105–109
87. Wang F, Liu X (2008) Upconversion multicolor fine-tuning: visible to near-infrared emission from lanthanide-doped NaYF4 nanoparticles. J Am Chem Soc 130(17):5642–5643
88. Wang F, Liu X (2009) Recent advances in the chemistry of lanthanide-doped upconversion nanocrystals. Chem Soc Rev 38(4):976–989
89. Ong LC, Gnanasammandhan MK, Nagarajan S, Zhang Y (2010) Upconversion: road to El Dorado of the fluorescence world. Luminescence 25(4):290–293
90. Qiu H, Chen G, Sun L, Hao S, Han G, Yang C (2011) Ethylenediaminetetraacetic acid (EDTA)-controlled synthesis of multicolor lanthanide doped BaYF5 upconversion nanocrystals. J Mater Chem 21(43):17202–17208
91. Yin A, Zhang Y, Sun L, Yan C (2010) Colloidal synthesis and blue based multicolor upconversion emissions of size and composition controlled monodisperse hexagonal NaYF4: Yb, Tm nanocrystals. Nanoscale 2(6):953–959
92. Yi G-S, Chow G-M (2007) Water-soluble NaYF4:Yb, Er(Tm)/NaYF4/polymer core/shell/shell nanoparticles with significant enhancement of upconversion fluorescence. Chem Mater 19(3):341–343
93. Liu C, Chen D (2007) Controlled synthesis of hexagon shaped lanthanide-doped LaF3 nanoplates with multicolor upconversion fluorescence. J Mater Chem 17(37):3875–3880
94. Wang L, Li Y (2006) Green upconversion nanocrystals for DNA detection. Chem Commun 24:2557–2559
95. Qin X, Yokomori T, Ju Y (2007) Flame synthesis and characterization of rare-earth (Er3+, Ho3+, and Tm3+) doped upconversion nanophosphors. Appl Phys Lett 90(7):073104
96. Heer S, Kömpe K, Güdel HU, Haase M (2004) Highly efficient multicolour upconversion emission in transparent colloids of lanthanide-doped NaYF4 nanocrystals. Adv Mater 16 (23–24):2102–2105
97. Yang J, Zhang C, Peng C, Li C, Wang L, Chai R, Lin J (2009) Controllable Red, green, blue (RGB) and bright white upconversion luminescence of Lu2O3:Yb3+/Er3+/Tm3+ nanocrystals through single laser excitation at 980 nm. Chem Eur J 15(18):4649–4655
98. Auzel F (2004) Upconversion and anti-stokes processes with f and d ions in solids. Chem Rev 104(1):139–174
99. Xu CT, Svensson N, Axelsson J, Svenmarker P, Somesfalean G, Chen G, Liang H, Liu H, Zhang Z, Andersson-Engels S (2008) Autofluorescence insensitive imaging using upconverting nanocrystals in scattering media. Appl Phys Lett 93(17):171103
100. Soukka T, Rantanen T, Kuningas K (2008) Photon upconversion in homogeneous fluorescence-based bioanalytical assays. Ann N Y Acad Sci 1130(1):188–200
101. Li C, Quan Z, Yang P, Huang S, Lian H, Lin J (2008) Shape-controllable synthesis and upconversion properties of lutetium fluoride (doped with Yb3+/Er3+) microcrystals by hydrothermal process. J Phys Chem C 112(35):13395–13404
102. Cheng L, Yang K, Li Y, Chen J, Wang C, Shao M, Lee S-T, Liu Z (2011) Facile preparation of multifunctional upconversion nanoprobes for multimodal imaging and dual-targeted photothermal therapy. Angew Chem 123(32):7523–7528
103. León-Luis SF, Rodríguez-Mendoza UR, Haro-González P, Martín IR, Lavín V (2012) Role of the host matrix on the thermal sensitivity of Er3+ luminescence in optical temperature sensors. Sens Actuators B Chem 174:176–186

104. Yi GS, Chow GM (2006) Synthesis of hexagonal-phase NaYF4:Yb, Er and NaYF4:Yb, Tm nanocrystals with efficient up-conversion fluorescence. Adv Funct Mater 16(18):2324–2329
105. Mai H-X, Zhang Y-W, Si R, Yan Z-G, Sun L-d, You L-P, Yan C-H (2006) High-quality sodium rare-earth fluoride nanocrystals: controlled synthesis and optical properties. J Am Chem Soc 128(19):6426–6436
106. Yi G-S, Chow G-M (2005) Colloidal LaF3:Yb, Er, LaF3:Yb, Ho and LaF3:Yb, Tm nanocrystals with multicolor upconversion fluorescence. J Mater Chem 15(41):4460–4464
107. Nabika H, Deki S (2003) Enhancing and quenching functions of silver nanoparticles on the luminescent properties of europium complex in the solution phase. J Phys Chem B 107 (35):9161–9164
108. Wang G, Peng Q, Li Y (2011) Lanthanide-doped nanocrystals: synthesis, optical-magnetic properties, and applications. Acc Chem Res 44(5):322–332
109. Demas JN, DeGraff BA (2001) Applications of luminescent transition platinum group metal complexes to sensor technology and molecular probes. Coord Chem Rev 211(1):317–351